Perspectives on oxide heterostructures – the curious case of γ-Al_2O_3/$SrTiO_3$

Christensen, Dennis Valbjørn

Published in:
Nanoscale

Link to article, DOI:
10.1039/D2NR07172J

Publication date:
2023

Document Version
Early version, also known as pre-print

Perspectives on Oxide Heterostructures – The Curious Case of γ-Al_2O_3/$SrTiO_3$

Dennis Valbjørn Christensen

Technical University of Denmark, Department of Energy Conversion and Storage, 2800 Kgs. Lyngby, Denmark

Abstract

The heterostructure formed by depositing nanoscale thin films of spinel γ-Al_2O_3 on perovskite $SrTiO_3$ exhibits a range of exciting properties including room temperature epitaxial growth, high electron mobility, strain-tunable magnetic order, and a symmetry-related reordering of the conduction bands. In comparison to the benchmark $LaAlO_3$/$SrTiO_3$ heterostructure, the γ-Al_2O_3/$SrTiO_3$ heterostructure has been more sparsely investigated, which leaves plenty of room for scientific and technological discoveries. In this perspective article, I describe the key findings of the γ-Al_2O_3/$SrTiO_3$ heterostructure and propose five directions for future research: 1) an exploration of novel phenomena emerging when relaxing the conventional epitaxial constraint of matching crystal structures across the interface, 2) a dynamic switching of a strong polarization through nanoscale electromigration of aluminum vacancies, 3) autonomous and forced enhancement of the electron mobility via oxygen vacancy diffusion, 4) writing and erasing of magnetic and conducting nanolines using ferroelastic domain walls, and 5) a multiferroic state formed by combining ferroelectricity, ferromagnetism, and ferroelasticity. The proposed research directions may shed light on both fundamental aspects of the heterostructure and pave the way for applications within green energy devices and nanoelectronics.

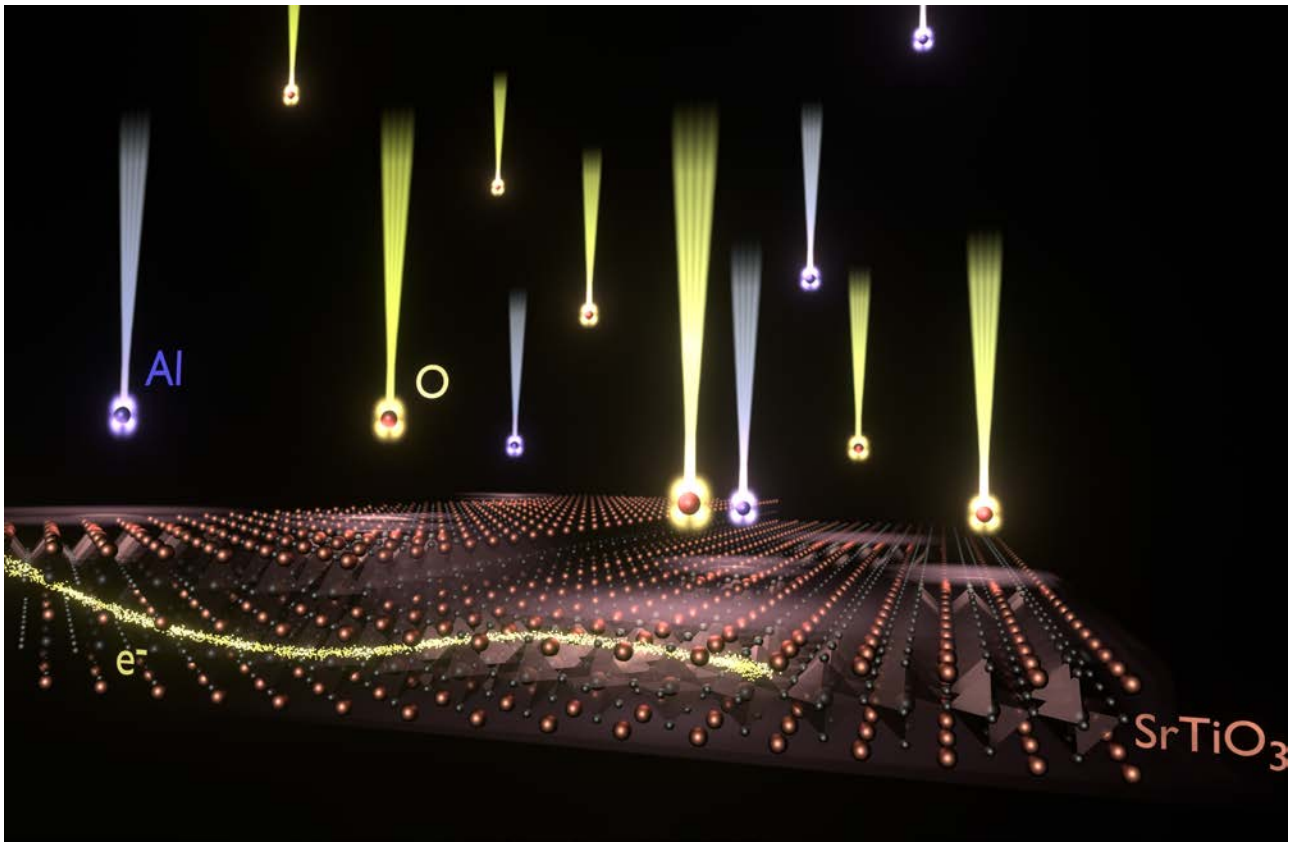

The strong market pull for high-speed and power-saving electronics has fueled the tremendous development in realizing faster, smaller, and more energy-efficient nanoelectronic devices. Two routes are used to satisfy this market pull: (i) Improving existing devices or (ii) designing devices with new functionalities. Appealing functionalities may be realized by using materials beyond the semiconducting materials that currently constitute the backbone of state-of-the-art electronic devices. A key example is the emergence of neuromorphic computation where non-volatile changes in the resistance observed on the nanoscale in, e.g., memristive oxides can be used to form a computational framework inspired by the human brain, which features both improved energy efficiency, learning capabilities and suitability for deep learning tasks [1]. A material system particularly rich in novel functionalities is the oxide heterostructure formed by depositing a nanoscale thin film of $LaAlO_3$ epitaxially on $SrTiO_3$ [2]. Despite both oxides being considered non-magnetic and insulating, conductivity and magnetism emerge at the interface along with numerous other functionalities [3]. In the wake of the large interest in the $LaAlO_3/SrTiO_3$ heterostructure, a new artificial system was obtained by replacing perovskite $LaAlO_3$ with spinel γ-Al_2O_3 [4]. The γ-$Al_2O_3/SrTiO_3$ heterostructure has shown to be an astonishing material platform in many ways, yet, the heterostructure has been much less studied compared to the benchmark $LaAlO_3/SrTiO_3$, which leaves plenty of room for future research adventures. Nonetheless, the heterostructure has already proven to possess several exciting properties not observed in the $LaAlO_3/SrTiO_3$ counterpart or in other $SrTiO_3$–based heterostructures. In this perspective article, I will first highlight some of the key findings that make the γ-$Al_2O_3/SrTiO_3$ heterostructure an exciting material platform to study, and secondly discuss several key opportunities for future research within nanoscale tailoring of this heterostructure.

Key findings:

Synthesis and electrical conductivity of γ-$Al_2O_3/SrTiO_3$:
The first remarkable characteristic of the γ-$Al_2O_3/SrTiO_3$ heterostructure is the possibility to grow the spinel γ-Al_2O_3 epitaxially on cubic perovskite $SrTiO_3$ using e.g. pulsed laser deposition and atomic layer deposition [5–7]. Typically, thin films of γ-Al_2O_3 with a thickness below 10 nm are deposited [5–7]. Despite the materials having different crystal structures, the oxygen sub-lattices are highly compatible, which enables the non-isomorphic epitaxial growth, even when depositing γ-Al_2O_3 at room temperature with pulsed laser deposition [4]. The matching oxygen sublattices are displayed in Figure 1a, which depicts $SrTiO_3$ capped with a generic spinel structure AB_2O_4 where aluminum occupies both A and B sites in the case of γ-Al_2O_3. The symmetry breaking at the spinel/perovskite interface is central to understanding the interface properties. For instance, when electrically insulating γ-Al_2O_3 is deposited on the insulating $SrTiO_3$, the resulting γ-$Al_2O_3/SrTiO_3$ heterostructure becomes conducting, and the itinerant electrons are confined at the interface by virtue of the broken symmetry [4,8]. The itinerant electrons confined to the interface live in a band structure that differs significantly from other $SrTiO_3$-based heterostructures due to the broken lattice symmetry [9,10]. From annealing in oxygen [11], high-temperature equilibrium conductance experiments [12], and numerical modeling [13] it is deduced that the itinerant electrons originate from oxygen vacancy donors formed in $SrTiO_3$ during the deposition. Hence, the origin of the itinerant electrons shares similarities to other $SrTiO_3$-based systems where amorphous or metal top layers such as Al are deposited on $SrTiO_3$ [14–16]. This origin raises an interesting paradox: The high-temperature equilibrium conductance measurements attribute the interface conductivity in $LaAlO_3/SrTiO_3$ to the $LaAlO_3$ polarity, but this is not the case for γ-$Al_2O_3/SrTiO_3$ although γ-Al_2O_3 has been considered polar [12]. Revisiting the atomic structure of γ-Al_2O_3, it was deduced that γ-Al_2O_3 can be non-polar for particular distributions of the aluminum vacancies that are intrinsically present in γ-Al_2O_3 [17].

Tunable electronic properties of γ-$Al_2O_3/SrTiO_3$:
Using the understanding of how the conductivity arises in γ-$Al_2O_3/SrTiO_3$, the carrier density can be tuned by controlling the oxygen vacancy concentration by varying the γ-Al_2O_3 deposition parameter [18] or performing post-annealing in oxygen at temperatures below 300 °C [11]. A similar tunability through defect engineering was also found in the heterostructure

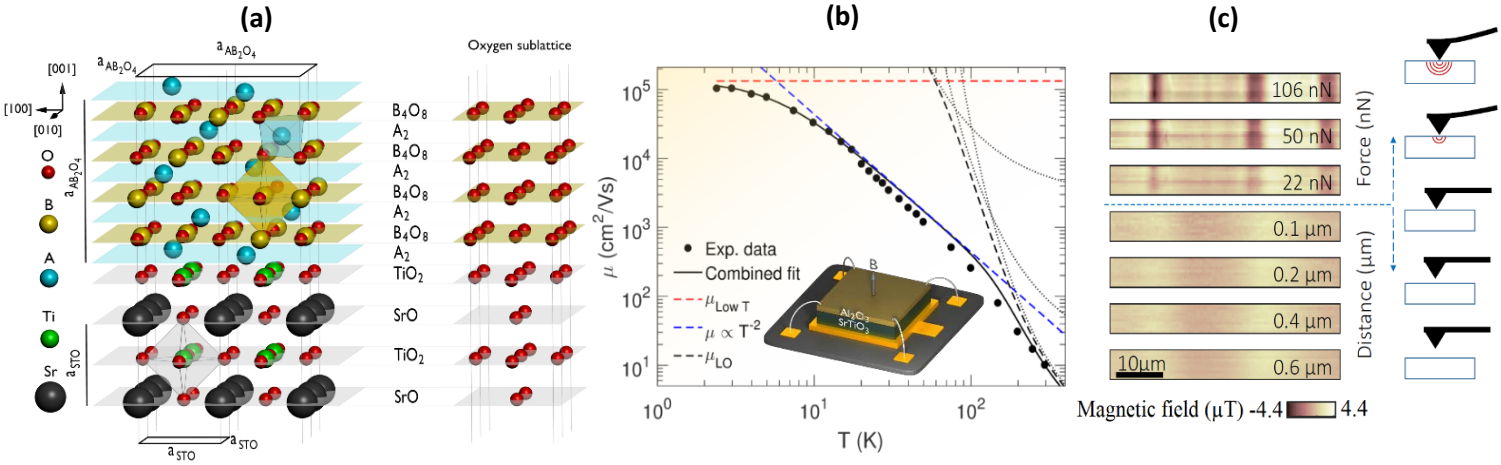

Figure 1 – Properties of the γ-$Al_2O_3/SrTiO_3$ heterostructure: *(a) Schematics of the crystal structure of the spinel/perovskite heterostructure where both A and B sites are occupied by aluminum with $2^2/_3$ aluminum vacancies pr. unit cell in the case of γ-Al_2O_3. Despite the different crystal structures, γ-Al_2O_3 can grow epitaxially on $SrTiO_3$ due to the compatible oxygen sublattice as depicted on the right-hand side. (b) Electron mobility (μ) as a function of temperature (T) including a fit using three different scattering contributions. (c) Scanning SQUID maps of the stray magnetic field above the γ-$Al_2O_3/SrTiO_3$ surface arising from magnetic order in the heterostructure as the probe is scanned in non-contact mode (lower 4 panels) and in contact mode with increasing pressure (upper 3 panels). The figures 1b and 1c are adapted from Ref. [21] and [21] with permission from American Physical Society and Springer Nature, respectively.*

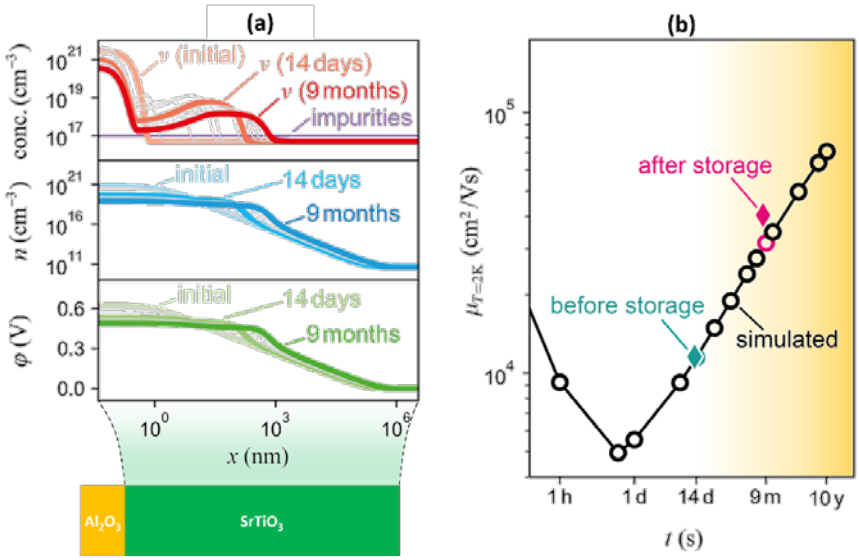

***Figure 2 – Self-enhancing electron mobility**: (a) Simulated depth-distribution of oxygen vacancy donors and background impurities (top) as well as itinerant electrons (middle) in a γ-Al_2O_3/$SrTiO_3$ heterostructure stored at room temperature for different periods after deposition. Here, x denotes the distance from the γ-Al_2O_3/$SrTiO_3$ interface. The electrostatic potential (bottom) associated with the oxygen vacancy distribution, which governs the distribution of itinerant electrons. (b) Simulated and measured electron mobility at 2 K ($\mu_{T=2K}$) for various storage times (t) after deposition of the γ-Al_2O_3/$SrTiO_3$ heterostructure. The figure are adapted from Ref. [25] with permission from American Physical Society.*

composed of amorphous $LaAlO_3$ deposited on $SrTiO_3$ where the electrons also originate from oxygen vacancies [11]. Electrons can also be induced in a non-volatile fashion using external stimuli on the macroscopic scale through conventional electrostatic gating [18], ionic liquid gating [19] or light exposure [18,20], and on the nanoscale using a biased atomic force microscopy tip [11]. The latter allows for a versatile patterning of circuits with nanoscale resolution [11].

Mechanically tunable magnetism:
Surprisingly, γ-Al_2O_3/$SrTiO_3$ was found to possess a mechanically tunable magnetic state [21]. The magnetic state manifests itself at T < 40 K both via the anomalous Hall effect and a magnetoresistance that deviates from Kohler's rule. Scanning SQUID was further used to detect a magnetic order extending hundreds of micrometers with modulations occurring along the tetragonal domain walls of $SrTiO_3$ (see Figure 1c). Applying force on the γ-Al_2O_3/$SrTiO_3$ surface using the scanning SQUID changes the magnetic order drastically, resulting in much stronger modulations (see Figure 1c). It was speculated that the applied force enhanced the magnetization by shifting the balance between the competition of a ferromagnetic order and a non-magnetic order. The ferromagnetic order is likely to arise from localized magnetic moments on oxygen vacancies that exchange couple to the itinerant electrons. The non-magnetic order may originate from, e.g., a singlet electron pairing as observed in a non-superconducting state for other $SrTiO_3$-based heterostructures [22–24].

Electron mobility:

At room temperature the electron mobility in γ-Al_2O_3/$SrTiO_3$ is generally found to be limited to 12 cm^2/Vs by phonon scattering [25], but with a few reports stating values exceeding 30 cm^2/Vs [26,27]. At 2 K the mobility exceeds 100,000 cm^2/Vs (see Figure 1b) at a high carrier density of ~$5 \cdot 10^{14}$ cm^{-2} [4,25], which differs fundamentally from bulk conducting $SrTiO_3$ and most other $SrTiO_3$-based heterostructures where high mobility is found at low carrier densities [28]. This mobility value at low temperatures is amongst the highest obtained for oxides [28].

The mobility in γ-Al_2O_3/$SrTiO_3$ can be enhanced by gentle post-annealing at ~100 °C or during prolonged room temperature storage [29]. The finite mobility of oxygen vacancies – acting both as electron donors and scattering centers – was attributed to being the cause of this self-enhancing mobility [13]. Drift-diffusion calculations were performed to describe the oxygen vacancy movement (see Figure 2). Here, part of the oxygen remained fixed at the γ-Al_2O_3/$SrTiO_3$ interface due to the broken lattice symmetry, whereas other oxygen vacancies formed a diffusion front that moved gradually deeper into the bulk of $SrTiO_3$ due to electrostatic repulsion (Figure 2a). The simulations further show that the resulting electrostatic potential from the charged oxygen vacancies caused a significant fraction of the electrons to be distributed between the interface and the diffusion front, thereby forming a high-way for high-mobility conduction in between the regions of high oxygen donor concentrations. A resulting self-enhancing electron mobility was predicted, which matched the experimental data well (Figure 2b). The high carrier density of ~$5 \cdot 10^{14}$ cm^{-2} is therefore predicted to be accompanied by a nanometric electron depth distribution after deposition to extending a micrometer or more into the $SrTiO_3$ substrate after prolonged aging for several months. This can be compared to experimental depth distributions extending 0.9 nm and 7.5 nm into $SrTiO_3$ as deduced from angle-dependent x-ray photoemission spectroscopy at room temperature and cryogenic infrared ellipsometry performed on samples without prolonged aging [4,8].

Future perspectives:

In contrast to the prototypical perovskite/perovskite $LaAlO_3$/$SrTiO_3$ interface, the spinel/perovskite γ-Al_2O_3/$SrTiO_3$ interface has been investigated more sparsely, which leaves plenty of room for exploring how the altered crystal structure across the interface may lead to unexpected phenomena. Below, I outline five key opportunities for future research inspired by the current knowledge of the γ-Al_2O_3/$SrTiO_3$ heterostructure:

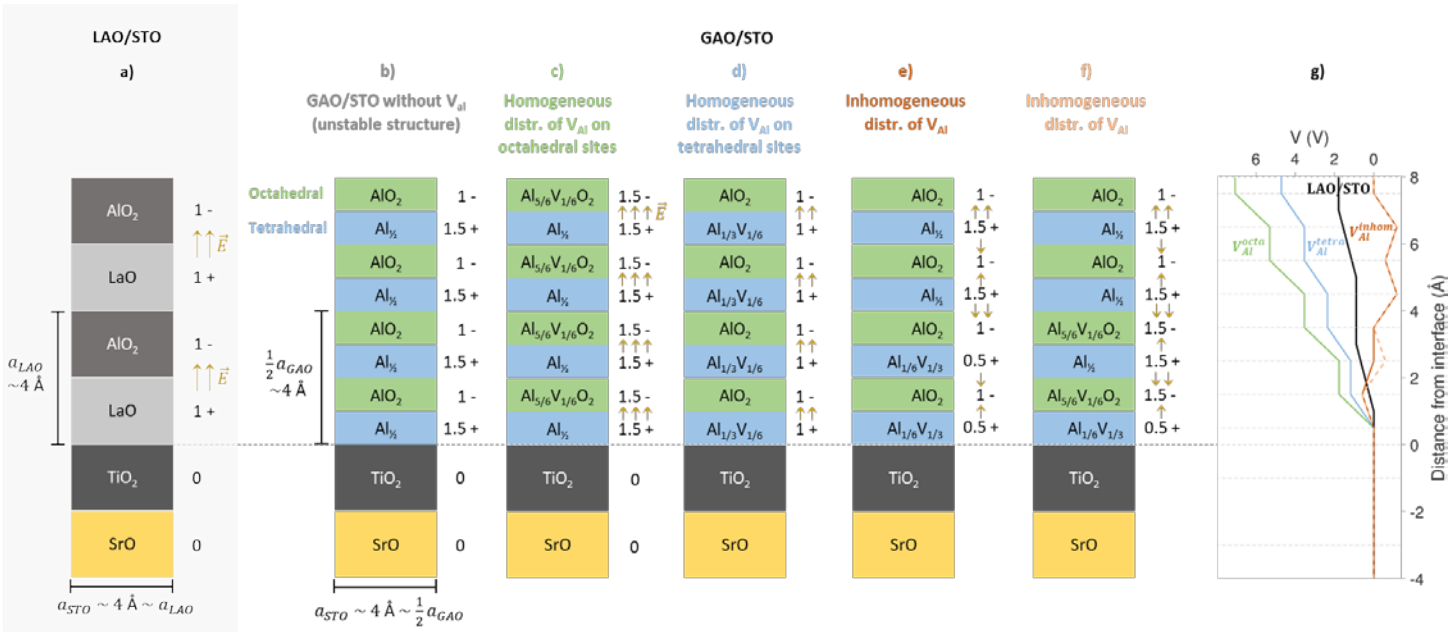

Figure 4 – Polarity in the γ-Al_2O_3/$SrTiO_3$ heterostructure: *(a) Schematics of the nominal polarity in $LaAlO_3$ deposited epitaxially on $SrTiO_3$ arising from polar ionic layers. (b-f) Schematics of the nominal polarity in γ-Al_2O_3 deposited epitaxially on $SrTiO_3$ if aluminum vacancies are (b) not present in the structure (charged structure), (c) present solely on octahedral sites, (d) present solely on tetrahedral sites, (e-f) distributed inhomogeneously to form overall non-polar states. (g) The electrostatic potential build-up due to the polarity as calculated by an electrostatic capacitor model. The figure is reproduced from Ref. [13] with permission from Elsevier.*

Broken lattice symmetry:

Conventional epitaxy relies on a high degree of structural coherency across the interface. Matching the crystal structure and lattice constant enables the growth of high-quality thin films using the substrate as a growth template. Broken symmetry is typically introduced by altering the composition of the constituent materials while still maintaining a reasonable match of the crystal structure across the heterointerface. Whereas high-quality homo- and heterostructures can be formed using this route, it imposes strict limitations on the choice of materials that can be combined. The γ-Al_2O_3/$SrTiO_3$ heterostructure partially relaxes these limitations by introducing broken symmetry from changing both the composition, lattice constant and crystal structure across the interface while still maintaining a high-quality epitaxial growth (see Figure 1a). A key example of how the broken symmetry at the perovskite/spinel interface influences the functional properties is the altered band structure. In (001)-oriented $LaAlO_3$/$SrTiO_3$, the bare $SrTiO_3$ surface as well as $SrTiO_3$ capped with Al metal, the lowest-lying band is of d_{xy} character, however, the presence of positively charged aluminum arranged in a spinel structure induces an increase in the d_{xy} energy so it shifts up above the level of the d_{xz} and d_{yz} bands in γ-Al_2O_3/$SrTiO_3$ [9,10,30–32].

It remains, however, largely unclear how other properties are influenced by transitioning from perovskite/perovskite to spinel/perovskite symmetries. In particular, the interesting electronic and magnetic properties originate from an interface-near region, making them susceptible to the lattice symmetry across the interface. The broken symmetry also influences the structural relaxation at the interface, which may form an interfacial polarization, emergent pyroelectricity and oxygen vacancy stabilization. In addition, it is of high interest to explore how the limitations of epitaxy can be further overcome not only by the non-isomorph epitaxial growth of different crystal structures but also by exploiting the recent progress within freestanding oxide thin films [33,34]. Using the latter approach, crystalline oxide thin films can be detached from the growth substrate and reunited with other films or substrates to form new interfaces not obtainable by conventional epitaxy (see Figure 4) [35]. Here, the high-quality epitaxial growth of γ-Al_2O_3 on perovskites may enable γ-Al_2O_3 to be used either as a sacrificial layer etchable with, e.g, NaOH [36] (blue layer in Figure 4) or as the active layer to be released from the substrate (yellow or red layer). This may enable high-quality spinel crystal structures with potentially sub-unit cell thicknesses to be released and subsequently recombined with other spinel or perovskite structures. The potential sub-unit cell release and recombination of 0.2 nm membranes (1/4 of a unit cell) allow for a larger surface-to-volume ratio as well as smaller building blocks

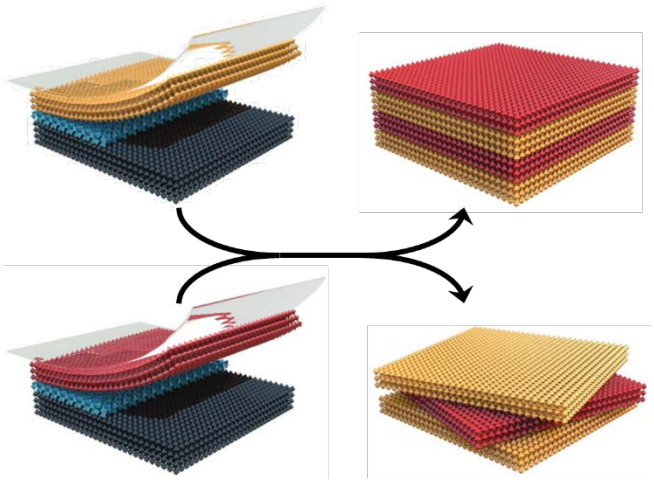

Figure 3 – Stacking and twisting of freestanding oxides: *An epitaxial heterostructure composed of a substrate (dark blue), sacrificial layer (light blue) and active layer (red and yellow) subjected to etching of the sacrificial layer can be used to detach the top layers from the growth substrate. This enables stacking of layers with different material classes (perovskites, spinels etc.) with a flexibility not allowed by conventional epitaxy. The figure is adapted from Ref. [29] with permission from Wiley.*

for the construction of stacked heterostructures. Of particular interest is the formation of conducting interfaces in heterostructures formed by stacking individual membranes. As the mechanism for forming conductivity in epitaxially grown γ-Al_2O_3/$SrTiO_3$ relies on the movement of oxygen across the interface, kinetic limitations may prevent conducting interfaces to be formed by room temperature stacking of non-conducting γ-Al_2O_3 and $SrTiO_3$ membranes. In contrast, conductivity may be formed by high-temperature reduction of $SrTiO_3$, which forms oxygen vacancy donors that can be kinetically trapped inside $SrTiO_3$ by a protective layer of γ-Al_2O_3. The new γ-Al_2O_3/$SrTiO_3$ interface may also serve to localize and thermodynamically stabilize oxygen vacancies at the interface.

Thickness-dependent dynamic polarity switching:

Beyond the potential polarity formed at the interface in γ-Al_2O_3/$SrTiO_3$, polarity may also form within the γ-Al_2O_3 layer. To obtain charge neutrality in γ-Al_2O_3, each spinel unit cell intrinsically contains $2^2/_3$ aluminum vacancies ($Al_{21⅓}O_{32}$) located on lattice sites with tetragonal and/or octahedral symmetries (see Figure 1a). Depending on the film thickness of γ-Al_2O_3 as well as the distribution of aluminum vacancies in γ-Al_2O_3, the film may either be highly polar or overall non-polar (Figure 3). By distributing the aluminum vacancies freely on tetragonal or octahedral sites, it was shown that no distributions of aluminum vacancies exist that give a non-polar film for thicknesses below one unit cell (0.8 nm corresponding to 8 sublayers) [4]. This should be compared to RHEED-monitored growth with sub-unit cell control of the thickness as 4 RHEED oscillations correspond to a single unit cell [4]. For a γ-Al_2O_3 thickness of 1 unit cell, the aluminum vacancies can either distribute in ways that produce a strong polarity (Figure 3c-d) or no overall polarity (Figure 3e-f) with a large predicted impact on the associated electrostatic potential build-up in the γ-Al_2O_3 layer (Figure 3g). A strong polarization of 75 μC/cm^2 is expected for aluminum vacancies distributed according to Figure 3c, which exceeds that found in single crystals of the strongly polar material $BaTiO_3$ (~25 μC/cm^2 [37]) as well as the spontaneous polarization at the surface of single-crystalline $SrTiO_3$ substrates (~5 μC/cm^2 [38]). A yet untested hypothesis exists suggesting that the polarity in γ-Al_2O_3 might be tunable by electric fields due to the electromigration of aluminum ions [17]. If disregarding the internal electrostatic build-up associated with the various cation configurations, the movement of aluminum vacancies is expected to have an activation barrier on the order of 0.6 eV for moving aluminum vacancies between lattice sites within γ-Al_2O_3 [39]. This is on the same order of magnitude as the barrier for oxygen vacancy diffusion in $SrTiO_3$ where electromigration is commonly observed [40,41]. This would offer switchable functionalities with similarities to conventional ferroelectrics, but with the switching caused by large-scale defect migration rather than small polar lattice distortions within a unit cell. In addition, the polarity may also be sensitive to applied stress and temperature, resulting in piezoelectric and pyroelectric properties.

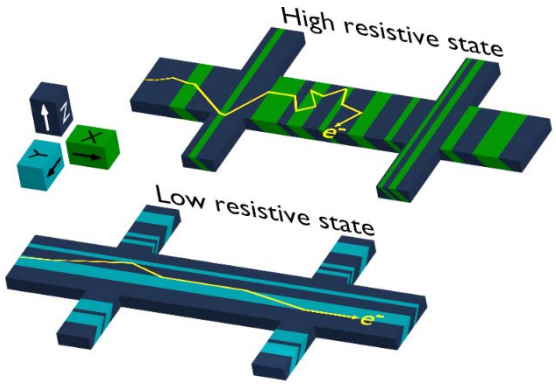

Figure 5 – Ferroelastic domain wall memristor: *Schematics of a ferroelastic domain wall memristor where external stimuli such as stress or electric fields may be used to control the landscape of ferroelastic domain walls and hence the resulting electrical resistivity in a non-volatile fashion.*

Self-enhancing electron mobility:

Oxygen vacancies in γ-Al_2O_3/$SrTiO_3$ serve key roles as electron dopants, scattering sites limiting the low-temperature mobility, and a likely source for magnetism. The diffusivity of oxygen vacancies in $SrTiO_3$ with an energy barrier on the order of 0.6 eV makes it possible for these key defects to move in absence of high temperatures. This stands in stark contrast to conventional electronic systems where donors are typically static, and it, therefore, opens up opportunities to tune functional properties through post-deposition treatment [11,42]. As mentioned above, it was suggested that the autonomous rearrangement of oxygen vacancies at room temperature resulted in a depth distribution, which favors high-mobility carriers [13]. One may expect that the diffusion can be changed from autonomous to controlled on-demand by adding an electric field from electrostatic gates to control the electromigration of oxygen vacancies. In this way, one can envision a dynamic control of both the location of electron donors as well as the resulting confinement potential and electron distribution in a non-volatile fashion. Back-gates are expected to primarily modulate the depth distribution of donors and vacancies whereas side gates or local gates from probes may control the lateral distribution as well. This is expected to have a strong impact on the electron mobility as well as other functional properties such as the magnetism observed in γ-Al_2O_3/$SrTiO_3$. The γ-Al_2O_3/$SrTiO_3$ interface here is expected to play the particular role of partially trapping the oxygen vacancies near the broken interface, which may be enhanced or diminished by replacing the γ-Al_2O_3 layer with other top films such as amorphous top layers [14], spinel layers with cation substitutions [43] or metal layers [16] to form a set of oxygen-deficient $SrTiO_3$–based heterostructures.

Writing functionalities with structural domain walls:

The magnetism and current distribution in γ-Al_2O_3/$SrTiO_3$ have stripy modulations at cryogenic temperatures aligned along the [100], [010], and [110] crystal directions [21,25]. The stripy features are attributed to the ferroelastic domains arising when $SrTiO_3$ transitions from cubic to tetragonal around 105 K. The

transition forms three different domains where the elongation of the tetragonal unit cell is along the x-, y-, and z-direction, respectively. This leads to a distribution of domains separated by domain walls where the spatial differences in the lattice here form modulations of the electronic and magnetic properties [21,25]. The size, number, and spatial distribution of domains and domain walls can be controlled using external stimuli such as mechanical stress and electric fields on both the macroscopic and microscopic scales [21,44]. This opens up for dynamically writing and erasing nanoscale lines with modified magnetic and conducting properties. As these lines are coupled to the underlying lattice structure, the changes are expected to be non-volatile, which may open up for designing spintronic devices and ferroelastic memristors (see Figure 5).

Multiferroicity:

As described above, $SrTiO_3$ turns ferroelastic below approximately 105 K. In addition, $SrTiO_3$ is a quantum paraelectric at cryogenic temperatures, which is characterized by the ferroelectric polarity of the unit cell being suppressed by quantum tunneling between two polar states, hence on average producing a non-polar state. As $SrTiO_3$ is on the verge of becoming a ferroelectric material, ferroelectricity can be induced by lattice modification such as applying stress [45], substituting Sr for Ca [46], or replacing ^{16}O with ^{18}O isotopes [47]. In addition, a ferromagnetic state appears to be formed as well in the γ-Al_2O_3/$SrTiO_3$ heterostructure [21]. This suggests that a multiferroic state awaits to be discovered in γ-Al_2O_3/$SrTiO_3$, which combines both ferroelastic, ferroelectric, and ferromagnetic properties in a single material system. Of particular interest would be to study to what extent the ferroelastic, ferroelectric, and ferromagnetic degrees of freedom couple together to form, e.g., magnetoelectric effects. Although this multiferroic state has yet to be observed in γ-Al_2O_3/$SrTiO_3$, several studies point to an intimate coupling between the spin, lattice and charge degrees of freedom as illustrated in Figure 6. Here, the magnetization is dynamically coupled to the lattice through its strain-tunable property as well as through its modulation on ferroelastic domain walls [21]. Similarly, the charge flow is also modulated by the ferroelastic domain walls [25]. Through an electron-phonon coupling, the charge further distorts the lattice to form a polaron with an enhanced effective mass as the charge flows in the structure [10]. Lastly, the spin and charge degrees of freedom are also coupled through the anomalous Hall effect and exchange coupling of spins with the itinerant charge carriers [21]. Whereas the ways these degrees of freedom couple together are not exclusive to γ-Al_2O_3/$SrTiO_3$ but rather occur in other $SrTiO_3$–based material systems as well [21,44,48–53], all coupled degrees of freedom have been observed in a single γ-Al_2O_3/$SrTiO_3$ sample. In addition, the coupling between charge and spin degrees of freedom through the anomalous Hall effect manifests itself in γ-Al_2O_3/$SrTiO_3$ as a strongly non-linear Hall resistance below a threshold temperature, which coincides with the emergence of a stripy modulation of the magnetic signal picked up by scanning magnetometry [21].

Conclusion:

The γ-Al_2O_3/$SrTiO_3$ heterostructure has already proven to be an exciting and multifunctional material system, which is less explored compared to the archetypical $LaAlO_3$/$SrTiO_3$ interface. Nonetheless, replacing the $LaAlO_3$ film with γ-Al_2O_3 results in, e.g., a severely broken lattice symmetry, reordering of the conduction band, and high electron mobility. I here propose to further expand the range of properties by 1) investigation of heterointerfaces not bound by conventional epitaxial constraints, 2) dynamic and thickness-dependent polarity switching, 3) electromigrative control of electron donors, 4) writing and erasing of conducting and magnetic nanolines, and 5) realization of co-existing ferroelasticity, ferromagnetism, and ferroelectricity in γ-Al_2O_3/$SrTiO_3$. This renders the material property an interesting material platform to explore for scientific purposes as well as for applications utilizing ferroelectricity, high-mobility electronics, and multiferroicity.

Acknowledgments:

D. V. C. acknowledges support from the Novo Nordic Foundation Nerd program, Grant No. NNF21OC0068015 (Superior)

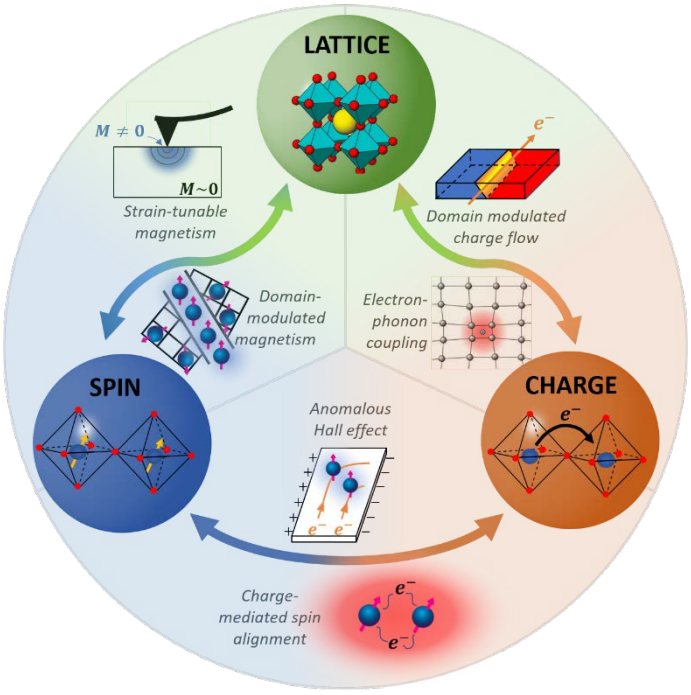

Figure 6 – Coupling of spin, lattice and charge degrees of freedom: *The wide range of properties observed in γ-Al_2O_3/$SrTiO_3$ arises due to the coupling of spin, lattice and charge degrees of freedom. The figure is adapted from Ref. [17] with permission from Springer Nature.*

References:

[1] D.V. Christensen, R. Dittmann, B. Linares-Barranco, A. Sebastian, M. Le Gallo, A. Redaelli, S. Slesazeck, T. Mikolajick, S. Spiga, S. Menzel, I. Valov, G. Milano, C. Ricciardi, S.-J. Liang, F. Miao, M. Lanza, T.J. Quill, S.T. Keene, A. Salleo, J. Grollier, D. Marković, A. Mizrahi, P. Yao, J.J. Yang, G. Indiveri, J.P. Strachan, S. Datta, E. Vianello, A. Valentian, J. Feldmann, X. Li, W.H.P. Pernice, H. Bhaskaran, S. Furber, E. Neftci, F. Scherr, W. Maass, S. Ramaswamy, J. Tapson, P. Panda, Y. Kim, G. Tanaka, S. Thorpe, C. Bartolozzi, T.A. Cleland, C. Posch, S. Liu, G. Panuccio, M. Mahmud, A.N. Mazumder, M. Hosseini, T. Mohsenin, E. Donati, S. Tolu, R. Galeazzi, M.E. Christensen, S. Holm, D. Ielmini, N. Pryds, 2022 roadmap on neuromorphic computing and engineering, Neuromorph. Comput. Eng. 2 (2022) 022501. https://doi.org/10.1088/2634-4386/ac4a83.

[2] A. Ohtomo, H.Y. Hwang, A high-mobility electron gas at the $LaAlO_3/SrTiO_3$ heterointerface, Nature. 427 (2004) 423–426.

[3] J.A. Sulpizio, S. Ilani, P. Irvin, J. Levy, Nanoscale Phenomena in Oxide Heterostructures, Annual Review of Materials Research. 44 (2014) 117–149. https://doi.org/10.1146/annurev-matsci-070813-113437.

[4] Y.Z. Chen, N. Bovet, F. Trier, D.V. Christensen, F.M. Qu, N.H. Andersen, T. Kasama, W. Zhang, R. Giraud, J. Dufouleur, T.S. Jespersen, J.R. Sun, A. Smith, J. Nygård, L. Lu, B. Büchner, B.G. Shen, S. Linderoth, N. Pryds, A high-mobility two-dimensional electron gas at the spinel/perovskite interface of γ-$Al_2O_3/SrTiO_3$, Nature Communications. 4 (2013) 1371. https://doi.org/10.1038/ncomms2394.

[5] Y.Z. Chen, N. Bovet, T. Kasama, W.W. Gao, S. Yazdi, C. Ma, N. Pryds, S. Linderoth, Room Temperature Formation of High-Mobility Two-Dimensional Electron Gases at Crystalline Complex Oxide Interfaces, Advanced Materials. 26 (2013) 1. https://doi.org/0.1002/adma.201304634.

[6] M. von Soosten, Dennis.V. Christensen, C.-B. Eom, Thomas.S. Jespersen, Y. Chen, N. Pryds, On the emergence of conductivity at $SrTiO_3$-based oxide interfaces – an in-situ study, Sci Rep. 9 (2019) 18005. https://doi.org/10.1038/s41598-019-54463-w.

[7] T.Q. Ngo, N.J. Goble, A. Posadas, K.J. Kormondy, S. Lu, M.D. McDaniel, J. Jordan-Sweet, D.J. Smith, X.P.A. Gao, A.A. Demkov, J.G. Ekerdt, Quasi-two-dimensional electron gas at the interface of γ-$Al_2O_3/SrTiO_3$ heterostructures grown by atomic layer deposition, Journal of Applied Physics. 118 (2015) 115303. https://doi.org/10.1063/1.4930575.

[8] M. Yazdi-Rizi, P. Marsik, B.P.P. Mallett, A. Dubroka, D.V. Christensen, Y.Z. Chen, N. Pryds, C. Bernhard, Infrared ellipsometry study of the confined electrons in a high-mobility γ-$Al_2O_3/SrTiO_3$ heterostructure, EPL (Europhysics Letters). 113 (2016) 47005. https://doi.org/10.1209/0295-5075/113/47005.

[9] Y. Cao, X. Liu, P. Shafer, S. Middey, D. Meyers, M. Kareev, Z. Zhong, J.-W. Kim, P.J. Ryan, E. Arenholz, J. Chakhalian, Anomalous orbital structure in a spinel–perovskite interface, Npj Quantum Materials. 1 (2016) 16009. https://doi.org/10.1038/npjquantmats.2016.9.

[10] A. Chikina, D.V. Christensen, V. Borisov, M.-A. Husanu, Y. Chen, X. Wang, T. Schmitt, M. Radovic, N. Nagaosa, A.S. Mishchenko, R. Valentí, N. Pryds, V.N. Strocov, Band-Order Anomaly at the γ-$Al_2O_3/SrTiO_3$ Interface Drives the Electron-Mobility Boost, ACS Nano. 15 (2021) 4347–4356. https://doi.org/10.1021/acsnano.0c07609.

[11] D.V. Christensen, M. von Soosten, F. Trier, T.S. Jespersen, A. Smith, Y. Chen, N. Pryds, Controlling the carrier density of $SrTiO_3$-based heterostructures with annealing, Advanced Electronic Materials. 3 (2017) 1700026.

[12] F. Gunkel, S. Hoffmann-Eifert, R.A. Heinen, D.V. Christensen, Y.Z. Chen, N. Pryds, R. Waser, R. Dittmann, Thermodynamic Ground States of Complex Oxide Heterointerfaces, ACS Applied Materials & Interfaces. 9 (2017) 1086–1092. https://doi.org/10.1021/acsami.6b12706.

[13] A.F. Zurhelle, D.V. Christensen, S. Menzel, F. Gunkel, Dynamics of the spatial separation of electrons and mobile oxygen vacancies in oxide heterostructures, Phys. Rev. Materials. 4 (2020) 104604. https://doi.org/10.1103/PhysRevMaterials.4.104604.

[14] Y. Chen, N. Pryds, J.E. Kleibeuker, G. Koster, J. Sun, E. Stamate, B. Shen, G. Rijnders, S. Linderoth, Metallic and Insulating Interfaces of Amorphous $SrTiO_3$-Based Oxide Heterostructures, Nano Letters. 11 (2011) 3774–3778. https://doi.org/10.1021/nl201821j.

[15] Q. Fu, T. Wagner, Metal/Oxide Interfacial Reactions: Oxidation of Metals on $SrTiO_3$ (100) and TiO_2 (110), The Journal of Physical Chemistry B. 109 (2005) 11697–11705. https://doi.org/10.1021/jp050601i.

[16] D.C. Vaz, E. Lesne, A. Sander, H. Naganuma, E. Jacquet, J. Santamaria, A. Barthélémy, M. Bibes, Tuning Up or Down the Critical Thickness in $LaAlO_3/SrTiO_3$ through In Situ Deposition of Metal Overlayers, Adv. Mater. 29 (2017) 1700486. https://doi.org/10.1002/adma.201700486.

[17] D.V. Christensen, A. Smith, Is γ-Al_2O_3 polar?, Applied Surface Science. 423 (2017) 887–890. https://doi.org/10.1016/j.apsusc.2017.06.184.

[18] D.V. Christensen, F. Trier, M. von Soosten, G.E.D.K. Prawiroatmodjo, T.S. Jespersen, Y.Z. Chen, N. Pryds, Electric field control of the γ-Al_2O_3/$SrTiO_3$ interface conductivity at room temperature, Applied Physics Letters. 109 (2016) 021602. https://doi.org/10.1063/1.4955490.

[19] W. Niu, Y. Zhang, Y. Gan, D.V. Christensen, M. von Soosten, E.J. Garcia-Suarez, A. Riisager, X. Wang, Y. Xu, R. Zhang, N. Pryds, Y. Chen, Giant Tunability of the Two-Dimensional Electron Gas at the Interface of γ-Al_2O_3/$SrTiO_3$, Nano Letters. 17 (2017) 6878.

[20] W. Niu, Y.-W. Fang, R. Liu, Z. Wu, Y. Chen, Y. Gan, X. Zhang, C. Zhu, L. Wang, Y. Xu, Y. Pu, Y. Chen, X. Wang, Fully Optical Modulation of the Two-Dimensional Electron Gas at the γ-Al_2O_3/$SrTiO_3$ Interface, J. Phys. Chem. Lett. 13 (2022) 2976–2985. https://doi.org/10.1021/acs.jpclett.2c00384.

[21] D.V. Christensen, Y. Frenkel, Y.Z. Chen, Y.W. Xie, Z.Y. Chen, Y. Hikita, A. Smith, L. Klein, H.Y. Hwang, N. Pryds, B. Kalisky, Strain-tunable magnetism at oxide domain walls, Nature Physics. 15 (2019) 269–274. https://doi.org/10.1038/s41567-018-0363-x.

[22] Y.-Y. Pai, A. Tylan-Tyler, P. Irvin, J. Levy, $LaAlO_3$/$SrTiO_3$: a tale of two magnetisms, in: Spintronics Handbook, Second Edition: Spin Transport and Magnetism, Second Edition, n.d.

[23] G. Cheng, M. Tomczyk, S. Lu, J.P. Veazey, M. Huang, P. Irvin, S. Ryu, H. Lee, C.-B. Eom, C.S. Hellberg, J. Levy, Electron pairing without superconductivity, Nature. 521 (2015) 196–199. https://doi.org/10.1038/nature14398.

[24] G.E.D.K. Prawiroatmodjo, M. Leijnse, F. Trier, Y. Chen, D.V. Christensen, M. von Soosten, N. Pryds, T.S. Jespersen, Transport and excitations in a negative-U quantum dot at the $LaAlO_3$/$SrTiO_3$ interface, Nature Communications. 8 (2017) 395. https://doi.org/10.1038/s41467-017-00495-7.

[25] D.V. Christensen, Y. Frenkel, P. Schütz, F. Trier, S. Wissberg, R. Claessen, B. Kalisky, A. Smith, Y.Z. Chen, N. Pryds, Electron Mobility in γ-Al_2O_3/$SrTiO_3$, Physical Review Applied. 9 (2018) 054004. https://doi.org/10.1103/PhysRevApplied.9.054004.

[26] K.H. Gao, X.R. Ma, Q.L. Li, X.H. Zhang, J.P. Xu, Y. Sun, G. Yu, High room temperature mobility in Al_2O_3/$SrTiO_3$ heterostructures, EPL. 138 (2022) 66003. https://doi.org/10.1209/0295-5075/ac74dd.

[27] M. Li, H. Yan, Z. Zhang, L. Ren, J. Zhao, S. Wang, C. Chen, K. Jin, Quasi-two-dimensional electron gas at γ-Al_2O_3/$SrTiO_3$ heterointerfaces fabricated by spin coating method, Journal of Applied Physics. 124 (2018) 145301. https://doi.org/10.1063/1.5047585.

[28] F. Trier, K.V. Reich, D.V. Christensen, Y. Zhang, H.L. Tuller, Y. Chen, B.I. Shklovskii, N. Pryds, Universality of electron mobility in $LaAlO_3$/$SrTiO_3$ and bulk $SrTiO_3$, Applied Physics Letters. 111 (2017) 092106. https://doi.org/10.1063/1.5001316.

[29] P. Schütz, D.V. Christensen, V. Borisov, F. Pfaff, P. Scheiderer, L. Dudy, M. Zapf, J. Gabel, Y.Z. Chen, N. Pryds, V.A. Rogalev, V.N. Strocov, T.-L. Lee, H.O. Jeschke, R. Valentí, M. Sing, R. Claessen, Microscopic origin of the mobility enhancement at a spinel/perovskite oxide heterointerface revealed by photoemission spectroscopy, Physical Review B. 96 (2017) 161409.

[30] N.C. Plumb, M. Radović, Angle-resolved photoemission spectroscopy studies of metallic surface and interface states of oxide insulators, J. Phys.: Condens. Matter. 29 (2017) 433005. https://doi.org/10.1088/1361-648X/aa833f.

[31] J.R.L. Mardegan, D.V. Christensen, Y.Z. Chen, S. Parchenko, S.R.V. Avula, N. Ortiz-Hernandez, M. Decker, C. Piamonteze, N. Pryds, U. Staub, Magnetic and electronic properties at the γ-Al_2O_3/$SrTiO_3$ interface, Physical Review B. 99 (2019). https://doi.org/10.1103/PhysRevB.99.134423.

[32] T.C. Rödel, F. Fortuna, S. Sengupta, E. Frantzeskakis, P.L. Fèvre, F. Bertran, B. Mercey, S. Matzen, G. Agnus, T. Maroutian, P. Lecoeur, A.F. Santander-Syro, Universal Fabrication of 2D Electron Systems in Functional Oxides, Advanced Materials. 28 (2016) 1976–1980. https://doi.org/10.1002/adma.201505021.

[33] D. Lu, D.J. Baek, S.S. Hong, L.F. Kourkoutis, Y. Hikita, H.Y. Hwang, Synthesis of freestanding single-crystal perovskite films and heterostructures by etching of sacrificial water-soluble layers, Nature Materials. 15 (2016) 1255–1260. https://doi.org/10.1038/nmat4749.

[34] F.M. Chiabrera, S. Yun, Y. Li, R.T. Dahm, H. Zhang, C.K.R. Kirchert, D.V. Christensen, F. Trier, T.S. Jespersen, N. Pryds, Freestanding Perovskite Oxide Films: Synthesis, Challenges, and Properties, Annalen Der Physik. 534 (2022) 2200084. https://doi.org/10.1002/andp.202200084.

[35] Y. Li, C. Xiang, F.M. Chiabrera, S. Yun, H. Zhang, D.J. Kelly, R.T. Dahm, C.K.R. Kirchert, T.E.L. Cozannet, F. Trier, D.V. Christensen, T.J. Booth, S.B. Simonsen, S. Kadkhodazadeh, T.S. Jespersen, N. Pryds, Stacking and Twisting of Freestanding Complex Oxide Thin Films, Advanced Materials. 34 (2022) 2203187. https://doi.org/10.1002/adma.202203187.

[36] N. Banerjee, G. Koster, G. Rijnders, Submicron patterning of epitaxial PbZr0.52Ti0.48O3 heterostructures, Applied Physics Letters. 102 (2013) 142909. https://doi.org/10.1063/1.4801776.

[37] J. Shieh, J.H. Yeh, Y.C. Shu, J.H. Yen, Hysteresis behaviors of barium titanate single crystals based on the operation of multiple 90° switching systems, Materials Science and Engineering: B. 161 (2009)

50–54. https://doi.org/10.1016/j.mseb.2008.11.046.
[38] E. Meirzadeh, D.V. Christensen, E. Makagon, H. Cohen, I. Rosenhek-Goldian, E.H. Morales, A. Bhowmik, J.M.G. Lastra, A.M. Rappe, D. Ehre, M. Lahav, N. Pryds, I. Lubomirsky, Surface Pyroelectricity in Cubic $SrTiO_3$, Advanced Materials. (2019) 1904733. https://doi.org/10.1002/adma.201904733.
[39] S.T. Murphy, B.P. Uberuaga, J.B. Ball, A.R. Cleave, K.E. Sickafus, R. Smith, R.W. Grimes, Cation diffusion in magnesium aluminate spinel, Solid State Ionics. 180 (2009) 1–8. https://doi.org/10.1016/j.ssi.2008.10.013.
[40] R. Waser, R. Dittmann, G. Staikov, K. Szot, Redox-Based Resistive Switching Memories - Nanoionic Mechanisms, Prospects, and Challenges, Advanced Materials. 21 (2009) 2632–2663. https://doi.org/10.1002/adma.200900375.
[41] J. Delahaye, T. Grenet, Gate voltage control of the $AlO_x/SrTiO_3$ interface electrical properties, Journal of Physics D: Applied Physics. 49 (2016) 395303. https://doi.org/10.1088/0022-3727/49/39/395303.
[42] A.V. Bjørlig, D.V. Christensen, R. Erlandsen, N. Pryds, B. Kalisky, Current Mapping of Amorphous $LaAlO_3/SrTiO_3$ near the Metal–Insulator Transition, ACS Appl. Electron. Mater. 4 (2022) 3421–3427. https://doi.org/10.1021/acsaelm.2c00264.
[43] Y. Zhang, Y. Gan, H. Zhang, H. Zhang, P. Norby, B. Shen, J. Sun, Y. Chen, Metallic conduction and ferromagnetism in $MAl_2O_4/SrTiO_3$ spinel/perovskite heterostructures (M = Fe, Co, Ni), Applied Physics Letters. 113 (2018) 261603. https://doi.org/10.1063/1.5063540.
[44] M. Honig, J.A. Sulpizio, J. Drori, A. Joshua, E. Zeldov, S. Ilani, Local electrostatic imaging of striped domain order in $LaAlO_3/SrTiO_3$, Nature Materials. 12 (2013) 1112–1118. https://doi.org/10.1038/nmat3810.
[45] J.H. Haeni, P. Irvin, W. Chang, R. Uecker, P. Reiche, Y.L. Li, S. Choudhury, W. Tian, M.E. Hawley, B. Craigo, A.K. Tagantsev, X.Q. Pan, S.K. Streiffer, L.Q. Chen, S.W. Kirchoefer, J. Levy, D.G. Schlom, Room-temperature ferroelectricity in strained $SrTiO_3$, Nature. 430 (2004) 758–761.
[46] J.G. Bednorz, K.A. Müller, $Sr_{1-x}Ca_xTiO_3$: An XY Quantum Ferroelectric with Transition to Randomness, Phys. Rev. Lett. 52 (1984) 2289–2292. https://doi.org/10.1103/PhysRevLett.52.2289.
[47] M. Itoh, R. Wang, Y. Inaguma, T. Yamaguchi, Y.J. Shan, T. Nakamura, Ferroelectricity induced by oxygen isotope exchange in strontium titanate perovskite, Physical Review Letters. 82 (1999) 3540.
[48] A. Vasudevarao, A. Kumar, L. Tian, J.H. Haeni, Y.L. Li, C.-J. Eklund, Q.X. Jia, R. Uecker, P. Reiche, K.M. Rabe, L.Q. Chen, D.G. Schlom, V. Gopalan, Multiferroic Domain Dynamics in Strained Strontium Titanate, Phys. Rev. Lett. 97 (2006) 257602. https://doi.org/10.1103/PhysRevLett.97.257602.
[49] Z. Wang, S. McKeown Walker, A. Tamai, Y. Wang, Z. Ristic, F.Y. Bruno, A. de la Torre, S. Riccò, N.C. Plumb, M. Shi, P. Hlawenka, J. Sánchez-Barriga, A. Varykhalov, T.K. Kim, M. Hoesch, P.D.C. King, W. Meevasana, U. Diebold, J. Mesot, B. Moritz, T.P. Devereaux, M. Radovic, F. Baumberger, Tailoring the nature and strength of electron–phonon interactions in the $SrTiO_3$(001) 2D electron liquid, Nature Materials. 15 (2016) 835–839. https://doi.org/10.1038/nmat4623.
[50] F. Gunkel, C. Bell, H. Inoue, B. Kim, A.G. Swartz, T.A. Merz, Y. Hikita, S. Harashima, H.K. Sato, M. Minohara, S. Hoffmann-Eifert, R. Dittmann, H.Y. Hwang, Defect Control of Conventional and Anomalous Electron Transport at Complex Oxide Interfaces, Physical Review X. 6 (2016) 031035. https://doi.org/10.1103/PhysRevX.6.031035.
[51] C. Cancellieri, A.S. Mishchenko, U. Aschauer, A. Filippetti, C. Faber, O.S. Barišić, V.A. Rogalev, T. Schmitt, N. Nagaosa, V.N. Strocov, Polaronic metal state at the $LaAlO_3/SrTiO_3$ interface, Nature Communications. 7 (2016) 10386. https://doi.org/10.1038/ncomms10386.
[52] B. Kalisky, E.M. Spanton, H. Noad, J.R. Kirtley, K.C. Nowack, C. Bell, H.K. Sato, M. Hosoda, Y. Xie, Y. Hikita, C. Woltmann, G. Pfanzelt, R. Jany, C. Richter, H.Y. Hwang, J. Mannhart, K.A. Moler, Locally enhanced conductivity due to the tetragonal domain structure in $LaAlO_3/SrTiO_3$ heterointerfaces, Nature Materials. (2013) 1091–1095. https://doi.org/10.1038/nmat3753.
[53] A. Joshua, J. Ruhman, S. Pecker, E. Altman, S. Ilani, Gate-tunable polarized phase of two-dimensional electrons at the $LaAlO_3/SrTiO_3$ interface, PNAS. 110 (2013) 9633–9638. https://doi.org/10.1073/pnas.1221453110.